An antagonistic driver of the microbial phyllosphere suppresses infection of *Arabidopsis thaliana* by the oomycete pathogen *Albugo laibachii* via a secreted hydrolase

Katharina Eitzen[1,2], Priyamedha Sengupta[1], Samuel Kroll[2], Eric Kemen*[2,3], Gunther Doehlemann*[1]

[1] *Institute for Plant Sciences and Cluster of Excellence on Plant Sciences (CEPLAS), University of Cologne, Center for Molecular Biosciences, Zuelpicher Str. 47a, 50674 Cologne, Germany.*

[2] *Max Planck Institute for Plant Breeding Research, Carl-von-Linne-Weg 10, 50829 Köln, Germany.*

[3] *Department of Microbial Interactions, IMIT/ZMBP, University of Tübingen, Tübingen, Germany*

* correspondence to:

Eric Kemen, eric.kemen@uni-tuebingen.de,

Gunther Doehlemann, g.doehlemann@uni-koeln.de

Short title: Microbial antagonism suppressing Albugo laibachii infection

Key words: microbial antagonism, plant pathogen, *Albugo laibachii*, Ustilaginales, Arabidopsis, transcriptomics, effectors

Abstract

In natural habitats, plants are challenged by pathogenic organisms, while they are extensively colonized by microbes, which establish a network of interactions with the plant and amongst each other. Therefore, plant immunity might not only be shaped by the co-evolutionary arms race between plants and pathogens, but also be a result from interactions within the microbiota and the host. In wild *Arabidopsis thaliana* populations, the oomycete pathogen *Albugo laibachii* has been identified as main driver of the phyllosphere microbiota. In this study, we describe the epiphytic yeast *Moesziomyces albugensis* and its antagonistic role in the microbial phyllosphere of *Arabidopsis thaliana*. *M. albugensis*, a close relative to pathogenic smut fungi, antagonizes several leaf-colonizing microbes. In particular, it prevents infection of *A. thaliana* by *A. laibachii*. Combination of transcriptomics and reverse genetics identified a gene of *M. albugensis* encoding a GH25 hydrolase as major factor of this microbial antagonism. Findings in this study provide identify a potential factor of oomycete biocontrol, provide mechanistic insight in microbial antagonism shaping leaf microbiota and provide new insights in the evolution of epiphytic basidiomycete yeasts.

Introduction

Plants are colonized by a wide range of microorganisms. While some microbes enter the plant and establish endophytic interactions with a broad range of outcomes from beneficial to pathogenic, plant surfaces harbor a large variety of microbial organisms. Recent research has focused largely on the importance of rhizoshpere microbiota in nutrient acquisition, pathogenic protection, and boosting overall plant growth and development [1–3]. However, the above ground parts of the plant including the phyllosphere are colonized by diverse groups of microbes that assist in plant protection and immunity [4,5] . The environment has a greater impact on the microbial community on the leaf surface, ultimately influencing the host-microbe interactions [6].

Scale-free network analysis was performed with the leaf microbial population of *Arabidopsis thaliana* [7]. Majority of the interactions existing in the network were found to be negative, consistent with the fact that it is rather the antagonistic interactions that stabilizes a microbial community [8]. Phyllosphere network analysis

of *A. thaliana* revealed a small number of microbes as hub organisms that have severe effect on the community structure. The major hub microbe in the *A. thaliana* phyllosphere is the oomycete *Albugo laibachii*, which is a biotrophic pathogen of Arabidopsis. This pathogen has been shown to significantly reduce the bacterial diversity of epiphytic and endophytic leaf habitats. Since bacteria generally comprises a large proportion of the phyllosphere microbiome, [9]; phylogenetic profiling of *A. thaliana* was also directed towards identifying a small group of bacteria that frequently colonize *A. thaliana* leaves. The analysis helped to develop a synthetic community of bacteria for gnotobiotic experiments.

Along with bacteria and oomycetes, a broad range of fungi are colonizers of the *A. thaliana* leaf. Among those fungi, basidiomycete yeasts are frequently found and the most frequent ones is the epiphytic basidiomycete genus *Dioszegia,* as well as an anamorphic yeast classified as Pseudozyma. sp. belonging to Ustilaginales [7]. This order comprises many pathogens of important crop plants, for example corn smut, loose smut of oats, barley and wheat are caused by *Ustilago maydis*, *U. avenae*, *U. nuda* and *U. tritici*, respectively. Ustilaginales *Pseudozyma* sp. yeasts, however are known to be devoid of any pathogenic sexual morph [10] and epiphytically colonize a wide range of habitats because of its rapid rate of asexual reproduction. Phylogenetic reconstruction [11] showed that the smut pathogen of millet, *Moesziomyces bullatus* and four species of *Pseudozyma*, namely *P. antarctica*, *P. aphidis*, *P. parantarctica* and *P. rugulosa* form a monophyletic group. The latter thus represent anamorphic and culturable stages of *M. bullatus* and can be transferred to this genus. *Moesziomyces strains* have been reported in a number of cases to act as microbial antagonists. *Pseudozyma aphidis* inhibited *Xanthomonas campestris* pv. *vesicatoria*, *X. campestris* pv. *campestris*, *Pseudomonas syringae* pv. *tomato*, *Clavibacter michiganensis*, *Erwinia amylovora*, and *Agrobacterium tumefaciens* in vitro and also led to the activation of induced defense responses in tomato against the pathogen ([12]). It was reported that *P. aphidis* can parasitize the hyphae and spores of *Podosphaera xanthii* [13]. *Pseudozyma churashimaensis* was reported to induce systemic defense in pepper plants against *X. axonopodis*, Cucumber mosaic virus, Pepper mottle virus, Pepper mild mottle virus, and Broad bean wilt virus [14].

In the present study, we explored the antagonistic potential of an anamorphic Ustilaginales yeast in the leaf microbial community of *A. thaliana*, where it prevents infection by the oomycete pathogen *A. laibachii.* In this pursuit, we identified

candidate genes in *M. albugensis*, which were upregulated in presence of *A. laibachii*, when both the microbes were co-inoculated in the host plant. Mutants of one of the candidates, belonging to Glycoside hydrolase – family 25 was found to lose its antagonistic abilities towards *A. laibachii,* providing mechanistic insight into fungal-oomycete antagonism in the leaf phyllosphere. Functional characterization of GH25 will be an important step towards establishing *M. albugensis* as a suitable microbial antagonist.

Results

In a previous study we reported that some microbes show a disproportional high impact on the plant-associated microbiota and that microbe-microbe interactions play a major role in phyllosphere networks [15]. Those disproportionately influential microbes we called “hubs”. From *Arabidopsis thaliana* leaves infected with the causal agent of white rust, *Albugo laibachii,* we isolated a basidiomycetous yeast. This yeast was tightly associated with *A. laibachii* spore propagation. Even after years of subculturing in the lab and re-inoculation of plants from frozen stocks of *A. laibachii* isolate Nc14, this yeast remained highly abundant in spore isolates. Phylogenetic analyses based on fungal ITS-sequencing identified the yeast as *Pseudozyma sp*. Those yeasts are a polyphyletic anamorphic genus which can be found across the family of Ustilaginaceae, a diverse group of basidiomycetous fungi, many of them known as pathogens of monocots like maize, barley, sugarcane or sorghum (Figure 1A and [16]). Microscopic analyses verified the morphological similarity between the putative *Pseudozyma sp*. and the Ustilaginaceous pathogen *Ustilago maydis*, the causal agent of corn smut disease which is an established model organism in fungal genetics and molecular plant pathology (Figure 1B;[16]). Based on phylogenetic similarity to the pathogenic smut *Moesziomyces bullatus* which infects millet, several anamorphic *Pseudozyma* isolates were suggested to be renamed and grouped to *M. bullatus* [11]. Since the new *Pseudozyma sp*. groups into the same cluster, we classified the newly identified species, which has been isolated from *A. laibachii* spores, as *Moesziomyces albugensis*.

Based on the identification of *M. albugensis* as a hub microbe in the *Arabidopsis* phyllosphere, we tested its interaction with 30 bacterial strains from 17 different species of a synthetic bacterial community (SynCom) of *Arabidopsis* leaves in one-to-one plate assays. This experiment identified seven strains being inhibited by

Moesziomyces, indicated by halo formation after 7 days of co-cultivation (Supplementary Figure S1). Interestingly, this inhibition was not seen when the pathogenic smut fungus *U. maydis* was co-cultivated with the bacteria, indicating a specific inhibition of the bacteria by *M. albugensis* (Supplementary Figure S1).

The primary hub microbe in the *Arabidopsis* phyllosphere was found to be the pathogenic oomycete *A. laibachii,* which was isolated in direct association with *Moesziomyces* [7]. To test if both species interfere with each other, we deployed a gnotobiotic plate system and quantified *A. laibachii* infection symptoms on *Arabidopsis*. In control experiments, spray inoculation of only *A. laibachii* spores to *Arabidopsis* leaves led to about 33% infected leaves at 14 dpi (Figure 2). In a next step, the bacterial SynCom was pre-inoculated to leaves two days before *A. laibachii* infection, which caused a significant reduction of *A. laibachii* infection by about 50% (Figure 2). However, if *Moesziomyces* was pre-inoculated with the bacterial SynCom, *A. laibachii* spore production was almost completely abolished. Similarly, the pre-inoculation of only *M. albugensis* resulted in an almost complete loss of *A. laibachii* infection, independently of the presence of a bacterial community (Figure 2). This demonstrates that *M. albugensis* holds a strong antagonistic activity towards *A. laibachii*, resulting in efficient biocontrol of pathogen infection.

The genome of *Moesziomyces albugensis.*

In light of its significant impact on both epiphytic bacteria and *A. laibachii,* we decided to characterize *M. albugensis* on genomic and genetic levels. Genome sequence of *M. albugensis* was analyzed by Single Molecule Real-Time sequencing (Pacific Biosciences, Menlo Park, CA), which lead to 69674 mapped reads with an accuracy of 87.3% and 8596bp sub-read length. Sequence assembly using the HGAP-pipeline (Pacific Biosciences) resulted in 31 Contigs with a N_{50}Contig Length of 705kb. The total length of all contigs results in a predicted genome size of 18.3Mb (Table 1). Gene prediction for the *M. albugensis* genome with Augustus [17] identified 6653 protein coding genes, of which 559 carry a secretion signal of which 380 are predicted to be secreted extracellularly (i.e. they do not carry membrane domains or cell-wall anchors) (Table 1). The small genome size and high number of coding genes results in a highly compact genome structure with only small intergenic regions. These are features similarly found in several pathogenic smut fungi such as *U. maydis* and *S. reilianum*, which also show similar genome sizes and gene

numbers (Table 1). Remarkably both *M. albugensis* and *Anthracocystis flocculosa,* which is another anamorphic and apathogenic yeast, show a similarly high rate of introns, while the pathogenic smut fungi have a significantly lower intron frequency (Table 1).

To get better insight in genome organization of *M. albugensis,* we compared its structure with the *U. maydis* genome, which serves as a manually annotated high-quality reference genome for smut fungi [18]. Out of the 31 *M. albugensis* contigs, 21 are showing telomeric structures and a high synteny to chromosomes of *U. maydis,* with three of them showing major events of chromosomal recombination (Figure 3A). Interestingly, the *Moesziomyces* contig 2, on which also homologs to pathogenic features like the *U. maydis* virulence cluster 2A [18] can be found, contains parts of three different *U. maydis* chromosomes (Chr. 2, 5, 20). The second recombination event on contig 6 affects the already studied *U. maydis* leaf specific effector *see1*, which is a virulence factor required for tumor formation [19]. This recombination event can also be found in the genome of the maize head smut *S. reilianum*, where the *U. maydis* chromosomes 5 and 20 recombined in the promoter region of the *see*1 gene (Figure 3B). In this respect it should be noted that *S. reilianum*, although infecting the same host, does not produce leaf tumors as *U. maydis* does [20]. Therefore, one could speculate if this difference might be reflected (or even caused) by this chromosomal rearrangement.

Also the third major recombination event, affecting *M. albugensis* contig 8, changes the genomic context of known effector genes with essential function for *U. maydis* virulence (*stp1* & *pit1/2*), as well as the A mating type locus, which is important for pheromone perception and recognition of mating partners. With respect to the strong antibiotic activities of *M. albugensis* we hypothesized the possible role of secondary metabolites. Using AntiSMASH identified 13 predicted secondary metabolite clusters in *M. albugensis,* of which three can be assigned to terpene synthesis, three contain non-ribosomal peptide synthases and one cluster has a polyketide synthetase as backbone genes (Supplementary Figure S2A). Interestingly, the secondary metabolite cluster which has been previously found in other Ustilaginomycetes to produce the antimicrobial metabolite Ustilagic acid, is absent in *M. albugensis* (Supplementary Figure S2B). On the contrary, we could identify three *M. albugensis* specific metabolite clusters which potentially could be involved in the antibacterial activity of *M. albugensis* (Supplementary Figure 2C).

Genome comparison of the related Ustilaginales yeast *A. flocculosa* with *U. maydis* reveals that this anamorphic strain has lost most of its effector genes, reflecting the absence of a pathogenic stage in this organism [21]. In contrast, *M. albugensis* contains 1:1 homologs of several known effectors with a known virulence function in *U. maydis* (Table 2). To functionally test a potential virulence activity of *M. albugensis* effector homologs, we expressed the homolog of the *U. maydis* core effector Pep1 in an *U. maydis* ∆pep1 deletion strain. This resulted in complete restoration of *U. maydis* virulence, demonstrating the presence of a functional effector in *M. albugensis* (Supplementary Figure S3).

A hallmark of the *U. maydis* genome structure was the finding of large gene clusters, which contain effector genes whose expression is induced only during plant infection [18]. To assess the presence of potential virulence clusters for *M. albugensis*, we compared all *U. maydis* effector gene clusters to the *M. albugensis* genome, based on homology. This showed that the twelve major effector clusters are present in *M. albugensis.* However, while many of the clustered effector genes are duplicated in pathogenic smut fungi, *M. albugensis* carries only a single copy of each effector gene, leading to minimal versions with strongly reduced gene numbers of all clusters (Supplemental Figure S4). This gets particularly obvious for the biggest and most intensively studied virulence cluster of smut fungi, the effector Cluster 19A [20,22,23]. In *M. albugensis* only three out of the 24 effector genes present in *U. maydis* are conserved in this cluster (Figure 4). Interestingly, some anamorphic yeasts like *Kalmanozyma brasiliensis* and *A. flocculosa* completely lost virulence clusters, while another non-pathogenic member of the Ustilaginales, *Pseudozyma hubeiensis,* shows an almost complete set of effectors when compared to *U. maydis* (Figure 4).

Genetic characterization of *M. albugensis*

To allow reverse genetics in *M. albugensis,* we enabled a genetic transformation system based on protoplast preparation and PEG-mediated DNA transfer. In a first step, transformants were generated by ectopic integration of a cytosolic expressed GFP reporter-gene under control of the constitutive *o2tef*-Promoter (Figure 5A). For the generation of knockout strains, a split marker approach was used to avoid ectopic integrations (Figure 5B). To allow generation of multiple knockouts, we used a selection marker cassette carrying a marker-recycling system [24], which uses self-

replicating plasmid (pFLPexpC) that carries an inducible flipper recombinase which cuts out the selection marker between two FRT-sites.

We decided to apply the transformation system to study the *M. albugensis* mating type loci in more detail. Although phylogenetically closely related to *U. hordei,* which has a bi-polar mating system, *M. albugensis* owns a tetrapolar mating system where both mating type loci are physically not linked. This situation is similar to the mating type structure in the pathogenic smut *U. maydis* (Figure 5A). The a-Locus, important for pheromone recognition, is located on contig 6, whereas the b-Locus can be found on contig 1. Since the *M. albugensis* genome is complete equipped in mating type genes, we first deployed a screen for potential mating partners. To this end, we screened wild *M. bullatus* isolates to find a suitable mating partner, but we could not observe a mating event (Supplementary Figure S5). To test if *M. albugensis* owns the ability to undergo pathogenic differentiation in the absence to a natural mating partner, we generated a self-compatible strain (CB1) which carries compatible b-mating alleles. To construct the CB1 strain, we used compatible alleles of the *bEast and bWest* genes of the barley smut *U. hordei*, which is the phylogenetically most closely related pathogen with for which genetic tools and detailed genetic information on mating type loci are available. The native *M. albugensis* locus was replaced by the compatible *U. hordei bEast* and *bWest* gene alleles via homologous recombination (Figure 6B).

Incubation of the *M. albugensis* CB1 on charcoal plates led to the formation of aerial hyphae, which generate the characteristic fluffy phenotype of filamentous strains also known from the self-compatible, solopathogenic *U. maydis* strains SG200 (Figure 6C). A second established method to induce filament formation in smuts is on hydrophobic parafilm [25]. Quantification after 18 hours incubation on parafilm resulted in filament formation of *M. albugensis* CB1 comparable to those of *U. maydis* strain SG200 (Figure 6D). While about 17% of *M. albugensis* wildtype cells showed filaments, the CB1 strain with compatible b-genes showed 38% filamentous growth.

While the switch from yeast-like growth to filamentous development is the first step in pathogenic development of smut fungi, host penetration is accompanied by the formation of a terminal swelling of infectious hyphae, termed “appressoria”. Induction of appressoria-formation *in vitro* was previously found to be induced by adding 100 µM of the cutin monomer 16-Hydroxyhexadecanoic acid (HDD) to the fungal cells prior to spraying onto a hydrophobic surface [25]. In absence of HDD, only about 8%

for *U. maydis* SG200 cells and 14% *M. albugensis* formed appressoria on parafilm at 24 hpi (Figure 6E). Addition of 100µM HDD resulted in significant induction of appressorium formation for both *U. maydis* and *M. albugensis*, demonstrating that *M. albugensis,* besides of its anamorphic lifestyle, does hold the genetic repertoire to form infection structures *in vitro*. Together, the analysis of the recombinant CB1 strain showed that *M. albugensis* can sense pathogenesis-related surface cues and produce penetration structures to a similar level as it is seen for the pathogenic model organism *U. maydis.*

Identification of microbe-microbe effector genes by RNA-Sequencing

To study the transcriptomic response of *M. albugensis* to different biotic interactions, RNA sequencing was performed. *M. albugensis* transcriptome was profiled in five different conditions (Figure 7A; cells in axenic culture versus cells on-planta, on-planta + SynCom, on-planta + *A. laibachii*, on-planta + SynCom + *A. laibachii*). Inoculation of *A. thaliana* leaves were done similar to the previously shown *A. laibachii* infection assays (Figure 7A). For *M. albugensis* RNA preparation, the epiphytic microbes were peeled from the plant tissue by using liquid latex (see methods section for details).

The libraries of 15 different samples (5 conditions in 3 biological replicates each) were generated by using a poly-A enrichment and sequenced on an Illumina HiSeq4000 platform. The paired end reads were mapped to the *M. albugensis* genome by using Tophat2 [26]. *M. albugensis* cells grown on *A. thaliana* (on-planta) showed 1300 downregulated and 1580 upregulated genes compared to axenic culture (Figure 7B and Table S1). Of the downregulated genes, 50% of all GO-terms are associated with primary metabolism (Supplementary Figure S6). In our test conditions we could see that in total 801 genes were upregulated in both *A. laibachii* condition. From those genes 411 genes were specific to incubation of *M. albugensis* with *A. laibachii* and our SynCom and 174 were specific to incubation with only *A. laibachii*. A set of 216 genes was shared with both conditions (Figure 7B and Table S1).

In presence of *A. laibachii,* mainly metabolism- and translation dependent genes were upregulated, which might indicate that *M. albugensis* can access a new nutrient source when being co-inoculated with *A. laibachii* (Supplementary Figure S6). From all *A. laibachii* – induced *M. albugensis* genes, 25 genes encode proteins carrying a

secretion signal peptide and having no predicted transmembrane domain (Figure 7C and Table S1). After excluding proteins being predicted to be located in intracellular organelles, nine candidate genes remained as potential microbe-microbe dependent effectors, i.e. *M. albugensis* genes being induced by *A. laibachii*, showing no or low expression in axenic culture and encode for proteins being predicted for extracellular secretion (Figure 7C and Table S1). Interestingly, four of these genes encode glycoside hydrolases. Furthermore, two genes encode peptidases, one gene encodes an alkaline phosphatase and two are uncharacterized proteins (Figure 7C and Table S1).

We selected two glycoside hydrolases *g5&g2490* (GH43 & GH25) and one uncharacterized protein (*g5755)* for gene deletion in *M. albugensis* to directly test their eventual function in the antagonism towards *A. laibachii*. The generated *M. albugensis* mutant strains were tested in a stress assay to check if the gene deletions resulted in general growth defects. Wild type and mutant *M. albugensis* strains were exposed to different stress components including osmotic stress (Sorbitol, NaCl), cell wall stress (Calcofluor, Congored) and oxidative stress (H_2O_2). Overall, this did not indicate a general growth defect of the tested deletion mutants in comparison to *M. albugensis*, wild type (Supplementary figure_S8). To test an eventual impact of the deleted genes in the antagonism of the two microbes, resulting *M. albugensis* deletion strains were inoculated to *A. thaliana* leaves prior to *A. laibachii* infection. Deletion of *g5* resulted in a significant but yet marginal increase of *A. laibachii* disease symptoms*,* while deletion of *g5755* had no effect on *A. laibachii*. We therefore considered these two genes being not important for the antagonism of *M. albugensis* towards *A. laibachii.* Strikingly, *M. albugensis*Δg2490 strains almost completely lost its biocontrol activity towards *A. laibachii,* which has been reproduced with similar results for two independents deletion strains (Figure 8A). To check if this dramatic loss of microbial antagonism is specific to the deletion of Δg2490, in-locus genetic complementation of strain Δg2490_1 was performed via homologous recombination. The resulting strain *M. albugensis*Δg2490/compl showed fully restored suppression of *A. laibachii* infection, confirming that the observed phenotype specifically resulted from the deletion of the g2490 gene (Figure 8B*)*. Together, these results demonstrate that the biocontrol of the pathogenic oomycete *A. laibachii* by the basidiomycete yeast *M. albugensis* is determined by the secretion of a previously

uncharacterized GH25 enzyme, which is transcriptionally activated specifically when both microbes are co-colonizing the *A. thaliana* leaf surface.

Discussion

Healthy plants in natural habitats are extensively colonized by microbes, therefore it has been hypothesized that the immune system and the microbiota may instruct each other beyond the simple co-evolutionary arms race between plants and pathogens [27]. Community members as individuals or in a community context have been reported to confer extended immune functions to their plant host. Root endophytic bacteria for example were found to protect *A. thaliana* and stabilize the microbial community by competing with filamentous eukaryotes [28]. A large inhibitory interaction network was found in the leaf microbiome of *A.thaliana* and used genome mining to identify over 1000 predicted natural product biosynthetic gene clusters (BGCs) [29]. In addition, the bacterium *Brevibacillus* sp. leaf 182 was found to inhibit half of the 200 strains isolated from *A. thaliana* phyllosphere. Further analysis revealed that *Brevibacillus* sp. leaf 182 produces a trans-acyltransferase polyketide synthase-derived antibiotic, macrobrevin along with other putative polyketide synthases [29].

In this study, we describe the role of the basidiomycete yeast *M*. *albugensis,* which we previously co-isolated with the oomycete pathogen *A. laibachii* and now characterized as an antagonistic driver in the *A. thaliana* phyllosphere. *A. laibachii* inhibits growth of seven members of a bacterial leaf SynCom and, most strikingly, it strongly suppresses disease progression and reproduction of the pathogenic oomycete *A. laibachii* on *A. thaliana*. *M. albugensis* is a member of the Ustilaginales, which previously has been classified to the pathogenic smut fungi of the *Moesziomyces bullatus* species [10]. Our genome analysis identified the anamorphic yeasts *M. rugulosus, M. aphidis* and *M. antarcticus*, which previously had been classified as "*Pseudozyma spec*." as closest relatives of *M. albugensis*. Anamorphic Ustilaginales yeasts are long known and have been used for biotechnological applications and also biocontrol [30]. Mannosylerythritol lipids produced by *M. antarcticus* are known to act as biosurfactants and are of great interest for pharmaceutical applications [31,32]. Glycolipids like Flocculosin produced by *A. flocculosa* or Ustilagic acid characterized in the smut fungus *U. maydis*, have

antifungal activity. Those compounds destabilize the membrane of different fungi and by this act as a biocontrol agent against powdery mildews or grey mold [33–35].

We identified 13 potential secondary metabolite clusters in *M*. *albugensis,* including non-ribosomal peptide synthases and polyketide synthetase. Interaction between microbes occupying the same habitat is believed to have given rise to a variety of secondary metabolites [36,37]. Presence of *Streptomyces rapamycinicus* activated an otherwise silent gene cluster, polyketide synthase, FgnA in *Aspergillus fumigatus.* The resultant compound was a potent fungal metabolite that in turn inhibited the spore-germination of *S. rapamycinicus* [38]. Therefore, the secondary metabolite gene clusters confer a competitive advantage to the fungi over the bacteria residing in the same environment.

What is still under debate is the relation of anamorphic yeasts with the related pathogenic smuts. Many smut fungi, including the model species *U. maydis* are dimorphic organisms. In their saprophytic phase they grow as haploid yeast cells, which are not infectious to plants. Only on appropriate host surfaces, haploid cells switch to filamentous growth and expression of pathogenicity-related genes is only activated upon mating in the filamentous dikaryon. A prime prerequisite for pathogenic development is therefore the ability of mating. Our genome analysis identified a tetrapolar mating system with a complete set of mating genes. Looking more closely on the phylogeny of different mating genes it appears that all sequenced *Moesziomyces* strains have the same pheromone receptor type (Supplementary Figure S7). Together with our mating tests which did not show mating for any *Moesziomyces* strains, this suggests that all sequenced strains of this species have the same mating type and due to that are not able to mate. Mating type bias after spore germination was reported for *Ustilago bromivora,* which leads to a haplo-lethal allele linked to the MAT-2 locus([39]). In this case, an intratetrad mating event rescues pathogenicity in nature as the second mating partner is not viable after spore germination. Together with the observation that anamorphic *Moesziomyces* yeasts can be found ubiquitous in nature one could hypothesize that those fungi are highly competitive in their haploid form which might have led to the selection for one viable mating type, which then adapted to the epiphytic life style.

Transcriptome analysis showed that epiphytic growth of *M. albugensis* on *A. thaliana* leads to massive transcriptional changes particularly in primary metabolism, which might reflect adaptation to the nutritional situation on the plant surface. Moreover, *M.*

albugensis showed specific transcriptional responses to a bacterial community, as well as to *A. laibachii* when being co-inoculated on plant leaves. Presence of *A. laibachii* resulted in an induction of primary metabolism and biosynthesis pathways, which might reflect elevated growth of *M. albugensis* in the presence of *A. laibachii.*

A set of *M. albugensis* genes encoding secreted hydrolases was induced by *A. laibachii* and one of these genes which encodes a putative GH25 hydrolase with similarity to *Chalaropsis* type lysozymes appeared to be essential for the biocontrol of *A. laibachii*. Initially discovered in the fungi *Chalaropsis* sp., this group of proteins is largely present in bacteria as well as phages for example the germination specific muramidase from *Clostridium perfringens* S40 [40]. The bacterial muramidase, cellosyl from *Streptomyces coelicolor* [41] also belongs to the *Chalaropsis* type of lysozyme. These proteins are proposed to cleave the β-1,4-glycosidic bond between N-acetylmuramic acid (NAM) and N-acetylglucosamine (NAG) in the bacterial peptidoglycan. Specifically, the β -1,4-N,6-O-diacetylmuramidase activity allows the *Chalaropsis* type lysozyme to degrade the cell walls of *Staphylococcus aureus*, in contrast to the commercially available Hen egg-white lysozyme (HEWL) [41]. The structure of Glycoside hydrolase family 25 from *Aspergillus fumigates* was characterized and the presence of N terminal signal peptide was considered to indicate an extracellular secretion of the protein with possible antimicrobial properties [42]. The role of the secreted hydrolase in the fungal kingdom is not completely explored yet. The presence of such hydrolases has in many cases been hypothesized to be associated with hyperparasitism of fungi parasitizing fungi [43] or oomycetes parasitizing oomycetes [44]. Our results might therefore indicate a cross kingdom hyperparasitism event between a fungus and an oomycete. Previous work on microbial communities has indicated that negative integrations stabilize microbial communities. Hyperparastitism is such a negative interaction with a strong eco-evolutionary effect on pathogen-host interactions and therefore on community stability [45]. *M. albugensis* might therefore regulate *A. laibachii* epidemics and reduce disease severity. As *A. laibachii* has been shown to reduce microbial diversity [7], *M. albugensis* might increase diversity through hyperparasitism of *A. laibachii*. At the same time this increased diversity might have caused the need for more secondary metabolites to evolve in the *M. albugensis* genome to defend against niche competitors. Through its close association with *A. laibachii*, *M. albugensis*

could be a key regulator of the *A. thaliana* microbial diversity and therefore relevant for plant health beyond the regulation of *A. laibachii* infection.

In conclusion, the secreted hydrolase we identified as main factor of *A. laibachii* inhibition has great potential to act as antimicrobial agent. The isolated compound is not only valuable in terms of ecological context. It can further lay the grounds for exploring other bioactive compounds produced in microbe-microbe interaction, especially the ones involved in plant protection. A main goal of our future studies will be to understand on the mechanistic level, how the GH-25 suppresses *A. laibachii*, and at which developmental step the oomycete infection is blocked. Since the GH-25 enzyme is well conserved amongst Ustilaginales including pathogenic species, it will also be tempting to elucidate, if there could a broadly conserved antagonism of Ustilaginales fungi and oomycetes, rather than a specific interaction of the two species we analyzed in this study. Functional investigation of these interactions can provide meaningful insights as to why certain yeasts prefer to colonize specific environments. At the same time, it will be worth exploring how the basidiomycete yeasts influence the bacterial major colonizers of the phyllosphere.

Material and Methods

Strains and Growth conditions

M. albugensis wildtype strain was isolated from *A. laibachii* infected *A. thaliana* leaves [7]. Wild-type *M. albugensis* (at 22 degrees) and *U. maydis* (at 28 degrees) strains were grown in liquid YEPSlight medium and maintained on Potato dextrose agar plates. King's B medium was used for culturing Syn Com bacterial members at 22 degrees. All the strains were grown in a rotary shaker at 200rpm. All the recipes for medium and solutions can be found in Supplementary Table S2. Stress assays for fungi: wildtype and mutant strains of *M. albugensis* grown to an optical density (600 nm) of 0.6-0.8 were centrifuged at 3500rpm for 10 minutes and suspended in sterile water to reach an OD of 1.0. Next, a dilution series from 10^0 to 10-4 was prepared in sterile H2O. In the end, 5 µl of each dilution are spotted on CM plates having components of different stress conditions. The plates are incubated for 2 days at 22°C. Confrontation assays: at first, *M. albugensis* and syncom bacterial strains are grown to an O.D of 0.8-1. *M. albugensis* cultures (10ul) are dropped in four quadrants of a Potato Dextrose Agar plate, spread previously with a bacterial culture. Plates are incubated for 2-4 days at 22°C.

Transformation of *M. albugensis*

Strains were grown in YEPSL at 22°C in a rotary shaker at 200rpm until an O.D. of 0.6 is reached and centrifuged for 15 mins at 3500rpm. The cells are washed in in 20 ml of SCS, and further centrifuged for 10 minutes at 3000rpm, before being treated with 3ml SCS solution with 20mg/ml of Glucanex (Lysing Enzyme from *Trichoderma harzianum*, # L1412, Sigma). After 20 minutes of incubation at room temperature, protoplasts start to come out from the cells. Cold SCS is added to the mix and spun down for 10 minutes at 2400rpm. The cells are washed twice with SCS and then resuspended with 10 ml STC to be centrifuged at 2000rpm for 10 minutes. Finally, the pellet is dissolved in 500 µl STC, and stored in aliquots of 50 µl at -80°C.5µg of plasmid DNA along with 15 µg Heparin was added to 50 µl protoplasts. After incubation on ice for 10 minutes, STC/40%PEG (500 µl) was added to it and mixed gently by pipetting up and down; this step was followed by another 15 minutes on ice. The transformation mix was added to 10 ml of molten regeneration (reg) agar and poured over a layer of already solidified reg agar containing appropriate antibiotic solution. For the bottom layer, we use 400 µg/ml Hygromycin/ 8 µg/ml Carboxin/ 300 µg/ml nourseothricin (NAT).

Knockout mutant generation and plasmid construction

Plasmids were cloned using *Escherichia coli* DH5α cells (Invitrogen, Karlsruhe, Germany). Construction of deletion mutants was performed by homologous recombination; the 5' and 3' flanking regions of the target genes were amplified and ligated to an antibiotic resistance cassette [46]. The ligated fragment was subsequently transformed into *M. albugensis*. Positive colonies for homologous integration were verified using colony PCR. Oligonucleotide pairs for knockout generation and verification can be found in Table S3. PCR amplification was done using Phusion© DNA polymerase (Thermo Scientific, Bonn, Germany), following the manufacturer's instructions, with 100 ng of genomic DNA or cDNA as template. Nucleic acids were purified from 1% TAE agarose gels using Macherey-Nagel™ NucleoSpin™ Gel and PCR Clean-up Kit.

Mating assay and generation of the self-compatible *M. albugensis* strain CB1

Haploid strains of *M. albugensis* were grown in liquid cultures, mixed and drops arranged on PD-plates with charcoal to induce filament formation. Plate with the haploid *Ustilago* strains FB1 and FB2 and the solopathogenic strain SG200 serve as internal control.

The complete b-locus of the solopathogenic *U. hordei* strain DS200 was amplified (Figure S2) and inserted into the *M. albugensis* b-locus by homologous recombination. The strain obtained, known as compatible b1 (CB1) was verified by amplification of the right border and left border areas with primers specific for the genomic locus and for the plasmid region. Additionally, two primers specific for the *M. albugensis bE*and *bW* genes were chosen to amplify parts of the native locus. To induce filament and appressoria formation in vitro we used a *Moesziomyces* YEPSL culture at OD_{600} 0.6-0.8. The cells were diluted to an OD_{600} of 0.2 in 2% YEPSL (for appressoria formation 100µM 16-hydroxyhexadecanoic acid or 1% ethanol was added) and sprayed the yeast like cells on parafilm which mimics the hydrophobic plant surface. After 18h incubation at 100% humidity the number of cells grown as filaments (or generating appressoria) was determined relative to the total number of total cells by using a light microscope.

Arabidopsis thaliana leaf infections

Sterilized *Arabidopsis thaliana* seeds were subjected to cold treatment for 7 days and sown on MS medium. The MS plates are directly transferred to growth chambers having 22°C on a short-day period (8 h light) with (37-40%) humidity and grown for 4 weeks before inoculation. Overnight liquid cultures of *M. albugensis* and Syn Com bacterial strains are grown to an OD_{600} of 0.6. The cultures are spun down at 3500rpm for 10 minutes and the pellets are dissolved in $MgCl_2$. 500µl of each culture is evenly sprayed on three-week old *A. thaliana* seedlings using airbrush guns. Two days later, spore solution of *A. laibachii* is then sprayed on the seedlings following the protocol of Ruhe et al. ([15]). Two weeks later, the disease symptoms on the leaves are scored as a percentage between infected and non-infected leaves.

Nucleic acid methods

RNA-Extraction of Latex-peeled samples: Four weeks old *A. thaliana* plants were fixed between two fingers and liquid latex was applied to the leaf surface by using a small brush. The latex was dried using the cold air option of a hair dryer, carefully

peeled off with a thin tweezer and immediately frozen in liquid nitrogen. Afterwards, the frozen latex pieces were grinded with liquid nitrogen and the RNA was isolated by using Trizol® Reagent (Invitrogen, Karlsruhe, Germany) according to the manufacturer's instructions. Turbo DNA-Free™ Kit (Ambion, life technologies™, Carlsbad, California, USA) was used to remove any DNA contamination in the extracted RNA. Synthesis of cDNA was performed using First Strand cDNA Synthesis Kit (Thermo Fischer scientific, Waltham, Massachusetts, USA) according to recommended instruction starting with a concentration of 10µg RNA. QIAprep Mini Plasmid Prep Kit (QIAGEN, Venlo, Netherlands) was used for isolation of plasmid DNA from bacteria after the principle of alkaline lysis. Genomic DNA was isolated using phenol-chloroform extraction protocol [18].

RT-qPCR oligonucleotide pairs were designed with Primer3 Plus. The oligonucleotide pairs were at first tested for efficiency using a dilution series of genomic DNA. The reaction was performed in a Bio-Rad iCycler system using the following conditions: 2 min at 95 °C, followed by 45 cycles of 30 s at 95 °C, 30 s at 61 °C and generation of melting curve between 65°C to 95°C.

Bioinformatics and computational data analysis

Sequence assembly of *M. albugensis* strains was performed using the HGAP pipeline (Pacific Biosciences). *M. albugensis* genome was annotated with the Augustus software tool. Secretome was investigated using SignalP4.0. Analysis of functional domains in the secreted proteins was done by Inter-Pro Scan. AntiSmash was used to predict potential secondary metabolite clusters. RNA sequencing was done at the CCG- Cologne Center for Genomics by using a poly-A enrichment on an Illumina HiSeq4000 platform. The achieved paired end reads were mapped to the *M. albugensis* and *A. thaliana* TAIR10 genome by using Tophat2 [26]. RNA-Seq reads of *M. albugensis* axenic cultures were used to generate exon and intron hints and to start a second annotation with Augustus. Heat-maps were performed using the heatmap.2 function of the package gplots (version 3.0.1) in r-studio (R version 3.5.1). An analysis of variance (ANOVA) model was used for pairwise comparison of the conditions, with Tukey's HSD test to determine significant differences among them (*P* values <0.05).

Data availability

Genome information and RNA sequencing have been submitted to NCBI Genbank and are available under the following links:https://www.ncbi.nlm.nih.gov/geo/query/acc.cgi?acc=GSE148670

Acknowledgments

This work was funded through by the Deutsche Forschungsgemeinschaft (DFG, German Research Foundation) under Germany's Excellence Strategy EXC-2048/1, Project ID 390686111, and the DFG priority program SPP2125 "DECRyPT". We are grateful to Marco Thines for generously providing *M. bullatus* wild type strains.

References

1. Ritpitakphong U, Falquet L, Vimoltust A, Berger A, Métraux JP, L'Haridon F. The microbiome of the leaf surface of Arabidopsis protects against a fungal pathogen. New Phytol. 2016. doi:10.1111/nph.13808
2. Walker TS, Bais HP, Grotewold E, Vivanco JM. Root exudation and rhizosphere biology. Plant Physiology. 2003. doi:10.1104/pp.102.019661
3. Bulgarelli D, Schlaeppi K, Spaepen S, van Themaat EVL, Schulze-Lefert P. Structure and Functions of the Bacterial Microbiota of Plants. Annu Rev Plant Biol. 2013. doi:10.1146/annurev-arplant-050312-120106
4. Busby PE, Peay KG, Newcombe G. Common foliar fungi of Populus trichocarpa modify Melampsora rust disease severity. New Phytol. 2016. doi:10.1111/nph.13742
5. Mikiciński A, Sobiczewski P, Puławska J, Maciorowski R. Control of fire blight (Erwinia amylovora) by a novel strain 49M of Pseudomonas graminis from the phyllosphere of apple (Malus spp.). Eur J Plant Pathol. 2016. doi:10.1007/s10658-015-0837-y
6. Stone BWG, Weingarten EA, Jackson CR. The Role of the Phyllosphere Microbiome in Plant Health and Function. Annual Plant Reviews online. 2018. doi:10.1002/9781119312994.apr0614
7. Agler MT, Ruhe J, Kroll S, Morhenn C, Kim ST, Weigel D, et al. Microbial Hub Taxa Link Host and Abiotic Factors to Plant Microbiome Variation. PLoS Biol. 2016. doi:10.1371/journal.pbio.1002352
8. Coyte KZ, Schluter J, Foster KR. The ecology of the mCoyte, K.Z., Schluter, J. & Foster, K.R. (2015) The ecology of the microbiome: Networks, competition, and stability. Science, 350, 663–666.icrobiome: Networks, competition, and stability. Science (80-). 2015. doi:10.1126/science.aad2602
9. Vorholt JA. Microbial life in the phyllosphere. Nature Reviews Microbiology. 2012. doi:10.1038/nrmicro2910
10. Kruse J, Doehlemann G, Kemen E, Thines M. Asexual and sexual morphs of Moesziomyces revisited. IMA Fungus. 2017.

doi:10.5598/imafungus.2017.08.01.09

11. Wang QM, Begerow D, Groenewald M, Liu XZ, Theelen B, Bai FY, et al. Multigene phylogeny and taxonomic revision of yeasts and related fungi in the Ustilaginomycotina. Stud Mycol. 2015. doi:10.1016/j.simyco.2015.10.004

12. Barda O, Shalev O, Alster S, Buxdorf K, Gafni A, Levy M. Pseudozyma aphidis induces salicylic-acid-independent resistance to Clavibacter michiganensis in tomato plants. Plant Dis. 2015. doi:10.1094/PDIS-04-14-0377-RE

13. Gafni A, Calderon CE, Harris R, Buxdorf K, Dafa-Berger A, Zeilinger-Reichert E, et al. Biological control of the cucurbit powdery mildew pathogen Podosphaera xanthii by means of the epiphytic fungus Pseudozyma aphidis and parasitism as a mode of action. Front Plant Sci. 2015. doi:10.3389/fpls.2015.00132

14. Lee G, Lee SH, Kim KM, Ryu CM. Foliar application of the leaf-colonizing yeast Pseudozyma churashimaensis elicits systemic defense of pepper against bacterial and viral pathogens. Sci Rep. 2017. doi:10.1038/srep39432

15. Ruhe J, Agler MT, Placzek A, Kramer K, Finkemeier I, Kemen EM. Obligate biotroph pathogens of the genus albugo are better adapted to active host defense compared to niche competitors. Front Plant Sci. 2016. doi:10.3389/fpls.2016.00820

16. Zuo W, Ökmen B, Depotter JRL, Ebert MK, Redkar A, Misas Villamil J, et al. Molecular Interactions Between Smut Fungi and Their Host Plants. Annu Rev Phytopathol. 2019. doi:10.1146/annurev-phyto-082718-100139

17. Stanke M, Steinkamp R, Waack S, Morgenstern B. AUGUSTUS: A web server for gene finding in eukaryotes. Nucleic Acids Res. 2004. doi:10.1093/nar/gkh379

18. Kämper J, Kahmann R, Bölker M, Ma LJ, Brefort T, Saville BJ, et al. Insights from the genome of the biotrophic fungal plant pathogen Ustilago maydis. Nature. 2006. doi:10.1038/nature05248

19. Redkar A, Hoser R, Schilling L, Zechmann B, Krzymowska M, Walbot V, et al. A secreted effector protein of Ustilago maydis guides maize leaf cells to form tumors. Plant Cell. 2015. doi:10.1105/tpc.114.131086

20. Schirawski J, Mannhaupt G, Münch K, Brefort T, Schipper K, Doehlemann G, et al. Pathogenicity determinants in smut fungi revealed by genome comparison. Science (80-). 2010. doi:10.1126/science.1195330

21. Lefebvre F, Joly DL, Labbé C, Teichmann B, Linning R, Belzile F, et al. The transition from a phytopathogenic smut ancestor to an anamorphic biocontrol agent deciphered by comparative whole-genome analysis. Plant Cell. 2013. doi:10.1105/tpc.113.113969

22. Brefort T, Tanaka S, Neidig N, Doehlemann G, Vincon V, Kahmann R. Characterization of the Largest Effector Gene Cluster of Ustilago maydis. PLoS Pathog. 2014. doi:10.1371/journal.ppat.1003866

23. Dutheil JY, Mannhaupt G, Schweizer G, Sieber CMK, Münsterkötter M, Güldener U, et al. A tale of genome compartmentalization: The evolution of

virulence clusters in smut fungi. Genome Biol Evol. 2016. doi:10.1093/gbe/evw026

24. Khrunyk Y, Münch K, Schipper K, Lupas AN, Kahmann R. The use of FLP-mediated recombination for the functional analysis of an effector gene family in the biotrophic smut fungus Ustilago maydis. New Phytol. 2010. doi:10.1111/j.1469-8137.2010.03413.x

25. Mendoza-Mendoza A, Berndt P, Djamei A, Weise C, Linne U, Marahiel M, et al. Physical-chemical plant-derived signals induce differentiation in Ustilago maydis. Mol Microbiol. 2009. doi:10.1111/j.1365-2958.2008.06567.x

26. Kim D, Pertea G, Trapnell C, Pimentel H, Kelley R, Salzberg SL. TopHat2: Accurate alignment of transcriptomes in the presence of insertions, deletions and gene fusions. Genome Biol. 2013. doi:10.1186/gb-2013-14-4-r36

27. Vannier N, Agler M, Hacquard S. Microbiota-mediated disease resistance in plants. PLoS Pathog. 2019. doi:10.1371/journal.ppat.1007740

28. Durán P, Thiergart T, Garrido-Oter R, Agler M, Kemen E, Schulze-Lefert P, et al. Microbial Interkingdom Interactions in Roots Promote Arabidopsis Survival. Cell. 2018. doi:10.1016/j.cell.2018.10.020

29. Helfrich EJN, Vogel CM, Ueoka R, Schäfer M, Ryffel F, Müller DB, et al. Bipartite interactions, antibiotic production and biosynthetic potential of the Arabidopsis leaf microbiome. Nat Microbiol. 2018. doi:10.1038/s41564-018-0200-0

30. Boekhout T. Pseudozyma Bandoni emend: Boekhout (1985) and a comparison with the yeast state of Ustilago maydis (De Candolle) Corda (1842). The Yeasts. 2011. doi:10.1016/B978-0-444-52149-1.00153-1

31. Kitamoto D, Akiba S, Hioki C, Tabuchi T. Extracellular accumulation of mannosylerythritol lipids by a strain of candida antarctica. Agric Biol Chem. 1990. doi:10.1080/00021369.1990.10869918

32. Morita T, Konishi M, Fukuoka T, Imura T, Kitamoto D. Microbial conversion of glycerol into glycolipid biosurfactants, mannosylerythritol lipids, by a basidiomycete yeast, Pseudozyma antarctica JCM 10317T. J Biosci Bioeng. 2007. doi:10.1263/jbb.104.78

33. Cheng Y, McNally DJ, Labbé C, Voyer N, Belzile F, Bélanger RR. Insertional mutagenesis of a fungal biocontrol agent led to discovery of a rare cellobiose lipid with antifungal activity. Appl Environ Microbiol. 2003. doi:10.1128/AEM.69.5.2595-2602.2003

34. Mimee B, Labbé C, Pelletier R, Bélanger RR. Antifungal activity of flocculosin, a novel glycolipid isolated from Pseudozyma flocculosa. Antimicrob Agents Chemother. 2005. doi:10.1128/AAC.49.4.1597-1599.2005

35. Teichmann B, Linne U, Hewald S, Marahiel MA, Bölker M. A biosynthetic gene cluster for a secreted cellobiose lipid with antifungal activity from Ustilago maydis. Mol Microbiol. 2007. doi:10.1111/j.1365-2958.2007.05941.x

36. Schroeckh V, Scherlach K, Nützmann HW, Shelest E, Schmidt-Heck W, Schuemann J, et al. Intimate bacterial-fungal interaction triggers biosynthesis

of archetypal polyketides in Aspergillus nidulans. Proc Natl Acad Sci U S A. 2009. doi:10.1073/pnas.0901870106

37. Rutledge PJ, Challis GL. Discovery of microbial natural products by activation of silent biosynthetic gene clusters. Nature Reviews Microbiology. 2015. doi:10.1038/nrmicro3496

38. Stroe MC, Netzker T, Scherlach K, Krüger T, Hertweck C, Valiante V, et al. Targeted induction of a silent fungal gene cluster encoding the bacteria-specific germination inhibitor fumigermin. Elife. 2020. doi:10.7554/eLife.52541

39. Rabe F, Bosch J, Stirnberg A, Guse T, Bauer L, Seitner D, et al. A complete toolset for the study of Ustilago bromivora and Brachypodium sp. as a fungal-temperate grass pathosystem. Elife. 2016. doi:10.7554/eLife.20522

40. Chen Y, Miyata S, Makino S, Moriyama R. Molecular characterization of a germination-specific muramidase from Clostridium perfringens S40 spores and nucleotide sequence of the corresponding gene. J Bacteriol. 1997. doi:10.1128/jb.179.10.3181-3187.1997

41. Rau A, Hogg T, Marquardt R, Hilgenfeld R. A new lysozyme fold. Crystal structure of the muramidase from Streptomyces coelicolor at 1.65 Å resolution. J Biol Chem. 2001. doi:10.1074/jbc.M102591200

42. Korczynska JE, Danielsen S, Schagerlöf U, Turkenburg JP, Davies GJ, Wilson KS, et al. The structure of a family GH25 lysozyme from Aspergillus fumigatus. Acta Crystallogr Sect F Struct Biol Cryst Commun. 2010. doi:10.1107/S1744309110025601

43. Hyde KD, Xu J, Rapior S, Jeewon R, Lumyong S, Niego AGT, et al. The amazing potential of fungi: 50 ways we can exploit fungi industrially. Fungal Diversity. 2019. doi:10.1007/s13225-019-00430-9

44. Horner NR, Grenville-Briggs LJ, van West P. The oomycete Pythium oligandrum expresses putative effectors during mycoparasitism of Phytophthora infestans and is amenable to transformation. Fungal Biol. 2012. doi:10.1016/j.funbio.2011.09.004

45. Parratt SR, Laine AL. The role of hyperparasitism in microbial pathogen ecology and evolution. ISME Journal. 2016. doi:10.1038/ismej.2015.247

46. Kämper J. A PCR-based system for highly efficient generation of gene replacement mutants in Ustilago maydis. Mol Genet Genomics. 2004. doi:10.1007/s00438-003-0962-8

47. Doehlemann G, Van Der Linde K, Aßmann D, Schwammbach D, Hof A, Mohanty A, et al. Pep1, a secreted effector protein of Ustilago maydis, is required for successful invasion of plant cells. PLoS Pathog. 2009. doi:10.1371/journal.ppat.1000290

48. Schilling L, Matei A, Redkar A, Walbot V, Doehlemann G. Virulence of the maize smut Ustilago maydis is shaped by organ-specific effectors. Mol Plant Pathol. 2014. doi:10.1111/mpp.12133

49. Seitner D, Uhse S, Gallei M, Djamei A. The core effector Cce1 is required for early infection of maize by Ustilago maydis. Mol Plant Pathol. 2018.

doi:10.1111/mpp.12698

50. Krombach S, Reissmann S, Kreibich S, Bochen F, Kahmann R. Virulence function of the Ustilago maydis sterol carrier protein 2. New Phytol. 2018. doi:10.1111/nph.15268

51. Schipper K. Charakterisierung eines Ustilago maydis Genclusters, das f€ur drei neuartige sekretierte Effektoren kodiert. PhDitle. PhD thesis. 2009.

52. Doehlemann G, Reissmann S, Aßmann D, Fleckenstein M, Kahmann R. Two linked genes encoding a secreted effector and a membrane protein are essential for Ustilago maydis-induced tumour formation. Mol Microbiol. 2011. doi:10.1111/j.1365-2958.2011.07728.x

53. Ma LS, Wang L, Trippel C, Mendoza-Mendoza A, Ullmann S, Moretti M, et al. The Ustilago maydis repetitive effector Rsp3 blocks the antifungal activity of mannose-binding maize proteins. Nat Commun. 2018. doi:10.1038/s41467-018-04149-0

54. Djamei A, Schipper K, Rabe F, Ghosh A, Vincon V, Kahnt J, et al. Metabolic priming by a secreted fungal effector. Nature. 2011. doi:10.1038/nature10454

55. Ökmen B, Kemmerich B, Hilbig D, Wemhöner R, Aschenbroich J, Perrar A, et al. Dual function of a secreted fungalysin metalloprotease in Ustilago maydis. New Phytol. 2018. doi:10.1111/nph.15265

Supporting information captions

Figure S1: Biocontrol activity of *M. albugensis* but not *U. maydis* against bacterial SynCom members [1]. Inhibiton by *Moesziomyces* can be seen by a characteristic halo formation after 48hrs of co-incubation.

Figure S2: (A)Predicted secondary metabolite clusters in the genome of *M. albugensis*. Most clusters are having unpredictable functions, three are each belonging to the type of terpene or nonribosomal peptide synthetase types and one is a polyketide synthetase cluster type I. (B) The gene cluster encoding for production of Ustilagicacid,a well-studied secondary metaboliteof smut fungi, is not present in the genome of *M. albugensis*. (C) Out of the 13 predicted secondary metabolite clusters clusters, three are unique to *M. albugensis*. Cluster 2 is predicted to encode a terpene, cluster 8 is a cluster of unkown function and cluster 10 is predicted as NRPS cluster. Core biosynthetic genes are highlighted in red, additional biosynthetic genes in yellow and transport related genes in blue, based on AntiSMASH predictions.

Figure S3: Protein alignment of the core effector Pep1 (Hemetsberger et al, 2015) from different Ustilaginomycetes (A). All characterized regions important for functionality are present in all different sequences. Deletion of the *pep1* gene (UMAG_01987) in *U. maydis* leads to complete loss of virulence, which can be restored by complementing the deletion mutant with the *M. albugensis pep1* gene (Ma1682). Infection of maize leaves was done as described in [2]. Disease symptoms were scored at 12 days post infection in three independent biological replicates. n= number of plants infected

Figure S4: Comparison of known virulence clusters [3] between *U. maydis* and *M. albugensis*. Numbers are gene numbers (*UMAG_NUMBER* for *U. maydis*; *gNUMBER* for *M. albugensis).*

Figure S5: Mating assays of *M. albugensis* and different *M. bullatus* isolates. Mixing of haploid *U. maydis* strains FB1 & FB2 and the solopathogenic strain SG200 served as a positive control for mating on charcoal plates, where filamentous growth is indicated by white, fluffy appearance of colonies. Haploid wild type strains without mating partner don't show a fluffy phenotype. For all combinations of *Moesziomyces* strains, no mating event resulting in filamentous growth on charcoal plates has been observed.

Figure S6: (A) Sequence distribution of Gene Ontology terms. 60% of all genes, downregulated in *M. albugensis* on plant compared to axenic culture growth, can be assigned to GO-terms related to metabolism and cell cycle. (B) In contrast, presence of *A. laibachii* leads to transcriptional activation of metabolic processes. 52% of all GO-terms associated with genes upregulated in presence of *A. laibachii* are related to metabolic processes.

Figure S7:A molecular phylogenetic analysis by maximum likelihood method based on pheromone receptor protein sequences. *M. albugensis* protein sequence clusters together with type 1 pheromone receptors of other Ustilaginomycetes.

Figure S8: Stress assay of *M. albugensis* wild type and knockout mutants of gene (g5,g5755 and g2490) respectively, on CM medium and 2% Glucose (A) with different conditions (B: 100 µg/ml Calcofluor; C: 150 µg/ml Calcoflour; D: 1 mMH2O2; E:45 µg/ml Congored; F: 1 M NaCl ; G: 1 M Sorbitol). The strains were dropped on the CM plates containing different stress supplements in a dilution series from 10^{0} to 10^{-4}

Figure Legends

Figure 1: Position of *M. albugensis* in the family of Ustilaginaceae. (A) molecular phylogenetic analysis by maximum likelihood method based on fungal ITS sequences shows *M. albugensis* grouping together with the millet pathogen *M. bullatus*. Pathogenic (green) and apathogenic species can be found across the phylogenetic tree. (B) Morphology of *M. albugensis* haploid cells grown in axenic culture compared to *U. maydis*, a well-studied pathogen of maize.

Figure 1: Infection assay of *A. laibachii* on *A. thaliana*. Addition of a bacterial SynCom reduces the infection symptoms of *A. laibachii* at 14dpi. Those symptoms can be almost abolished by spraying *M. albugensis* to the plant, whose biocontrol ability is directly targeting the oomycete pathogen. An analysis of variance (ANOVA) model was used for pairwise comparison of the conditions, with Tukey's HSD test to determine significant differences among them (P values <0.05).

Figure 2:Circos comparison of *M. albugensis* and *U. maydis* chromosome structure (A). We highlighted potential secondary metabolite clusters, secreted proteins and gene predictions on both strands (+/-). Homology based comparisons showed three chromosomal recombination events (B), which affects the *M. albugensis* contigs 2, 6 & 8.

Figure 3: Structure of the biggest virulence cluster (Cluster 19A) in pathogenic and non-pathogenic smut fungi. Colors indicate genes showing homology to each other related gene families are indicated in orange, yellow, blue, green and brown, whereas unique effector genes are shown in grey. Genes encoding proteins without a secretion signal are shown in white ([22]).

Figure 4: Genetic transformation of *M. albugensis* (A) Stable transformants could be achieved by first generating protoplasts with Glucanex and afterwards integrating linear DNA-fragments ectopically into the genome via PEG-mediated transformation. With this method we could generate a hygromycin resistant GFP-marker strain. (B) A

split-marker approach was used to generate deletion mutants via homologous recombination.

Figure 5: The self-compatible *M. albugensis* strain CB1 (A) *M. albugensis* mating type genes can be found on two different chromosomes similar to the tetrapolar mating type system in *U. maydis*. (B) To generate a self-compatible strain, we used the b-mating genes of *U. hordei* and integrated them at the native *M. albugensis* locus. (C) Strain CB1 shows a fluffy phenotype on charcoal plates and filamentous growth. (D,E) Induction of filamentation and appressoria formation in strain CB1. After incubation on a hydrophobic surface, both, filament and appressoria formation were significantly different (* Chi-Square Test for Independence – p = 0,0001) when compared to *M. albugensis* wildtype and similar to the level of the self-compatible *U. maydis* strain SG00 [18].

Figure 6: Transcriptome analysis of *M. albugensis* (A) Experimental setup and selected conditions to identify microbe-microbe dependent genes by RNA-Sequencing in *M. albugensis*. (B) Venn diagrams showing differential regulated *M. albugensis* genes after spraying of haploid cells to the *A. thaliana* leaf surface leads.1300 down- and 1580-upregulated genes and resemble the transcriptional response of *Moesziomyces* to the plant surface only. A total number of 801 genes upregulated in response to the presence of *A. laibachii* and 216 of those genes are upregulated in both conditions. (C) Hierarchical clustering of the 27 *A. laibachii* -induced *M. albugensis* genes being predicted to encode secreted proteins. Of these candidate genes, nine were selected identified as candidate microbe-microbe effectors, based on their transcriptional regulation and prediction to encode for extracellularly localized proteins.

Figure 7: Reverse-genetic identification of an *M. albugensis* gene which is responsible for the suppression of *A. laibachii* infection. Test of *M. albugensis* deletion mutants of potential microbe-microbe dependent regulated genes in Arabidopsis leaf infections with *A. laibachii*. (A) Three candidate genes (*g5*, *g5755* & *g2490*) were deleted in *M. albugensis* and deletion strains were individually

inoculated on *A. thaliana* together with *A. laibachii*. Inoculation of two independent strains being deleted for *g2490 (Δg2490_1; Δg2490_2)* resulted in significant and almost complete loss the biocontrol activity of *M. albugensis*. While deletion of g5 resulted in a marginal reduction of disease symptoms, deletion of g5755 had no effect on *A. laibachii.* (B) Genetic complementation of the *g2490* deletion restores the biocontrol activity to wildtype levels.

Tables

Table 1: Comparison of Genomes and genomic features of known pathogenic and apathogenic Ustilaginomycetes.

	M. albugensis	*U. bromivora*	*S. scitamineum*	*S. reilianum*	*U. maydis*	*U. hordei*	*M. pennsylvanicum*	*A. flocculosa*
Assembly statistics								
Total contig length (Mb)	18.3		19.5	18.2	19.7	20.7	19.2	23.2
Total scaffold length (Mb)		20.5	19.6	18.4	19.8	21.15	19.2	23.3
Average base coverage	50x	154x	30x	20x	10x	25x	339x	28x
N50 contig (kb)	705.1		37.6	50.3	127.4	48.7	43.4	38.6
N50 scaffold length (kb)		877	759.2	738.5	817.8	307.7	121.7	919.9
Chromosomes	21	23		23	23	23		
GC-content (%)	60.9	52.4	54.4	59.7	54	52	50.9	65.1
Coding (%)	62.8	54.4	57.8	62.6	56.3	54.3	54	66.3
Coding Sequence								
Percentage CDS (%)	69.5	59.8	62	65.9	61.1	57.5	56.6	54.3
Average gene size (bp)	1935	1699	1819	1858	1836	1708	1734	2097
Average gene density (gene/kb)	0.36	0.35	0.34	0.37	0.34	0.34	0.33	0.30
Protein-coding genes	6653	7233	6693	6648	6786	7113	6279	6877
Exons	11645	11154	10214	9776	9783	10907	9278	19318
Average exon size (bp)	1091	1101	1191	1221	1230	1107	527	658
Exons/gene	1.75	1.5	1.5	1.47	1.44	1.53	1.48	2.8
tRNA genes	150	133	116	96	111	110	126	176
Noncoding sequence								
Introns	9333	3921	3521	3103	2997	3161	2999	12427
Introns/gene	1.40	0.54	0.53	0.47	0.44	0.44	0.48	1.81
Average intron length (base)	163	163	130.1	144	142	141	191.4	141
Average intergenic distance (bp)	769	1054	1114	929	1127	1186	1328	1273
Secretome								
Protein with signal peptide	559		622	632	625	538	419	622
Secreted without TMD	380				467			737
- with known domain	260				264			554

[23,39]

Table 2: *M. albugensis* proteins homologous to *U. maydis* effector genes with known virulence function.

Name	Homologue	Query cover	E-value	Identity (%)	*U. maydis* knockout phenotype	Reference
g1653	UMAG_01987 (Pep1)	82%	3-e56	60.96	complete loss of tumor formation - blocked in early stages of infection	[47]
g1828	UMAG_01829 (Afu1)	99%	0.0	71.57	organ specific effector - reduced virulence in seedling leaves	[48]
g2626	UMAG_12197 (Cce1)	98%	1e-48	60.16	complete loss of tumor formation - blocked in early stages of infection	[49]
g2765	UMAG_11938 (Scp2)	100%	1e-73	93.44	Reduced in virulence	[50]
g2910	UMAG_02475 (Stp1)	32%	3e-42	60.71	complete loss of tumor formation - blocked in early stages of infection	[51]
g3652	UMAG_02239 (See1)	43%	9e-11	54.90	organ specific effector - reduced virulence in seedling leaves	[19]
g3113	UMAG_01375 (Pit2)	*	*	*	complete loss of tumor formation - blocked in early stages of infection	[52]
g3279	UMAG_03274 (Rsp3)	10%	5e-20	70.11	strong attenuation of virulence – reduced tumor size and number	[53]
g5296	UMAG_05731 (Cmu1)	98%	3e-70	43.84	Reduced virulence	[54]
g6183	UMAG_06098 (Fly1)	100%	0.0	81.85	Reduced virulence	[55]
g5835	UMAG_05302 (Tin2)	87%	8e-24	37.81	Minor impact on tumor formation – reduced anthocyanin biosynthesis	[22]

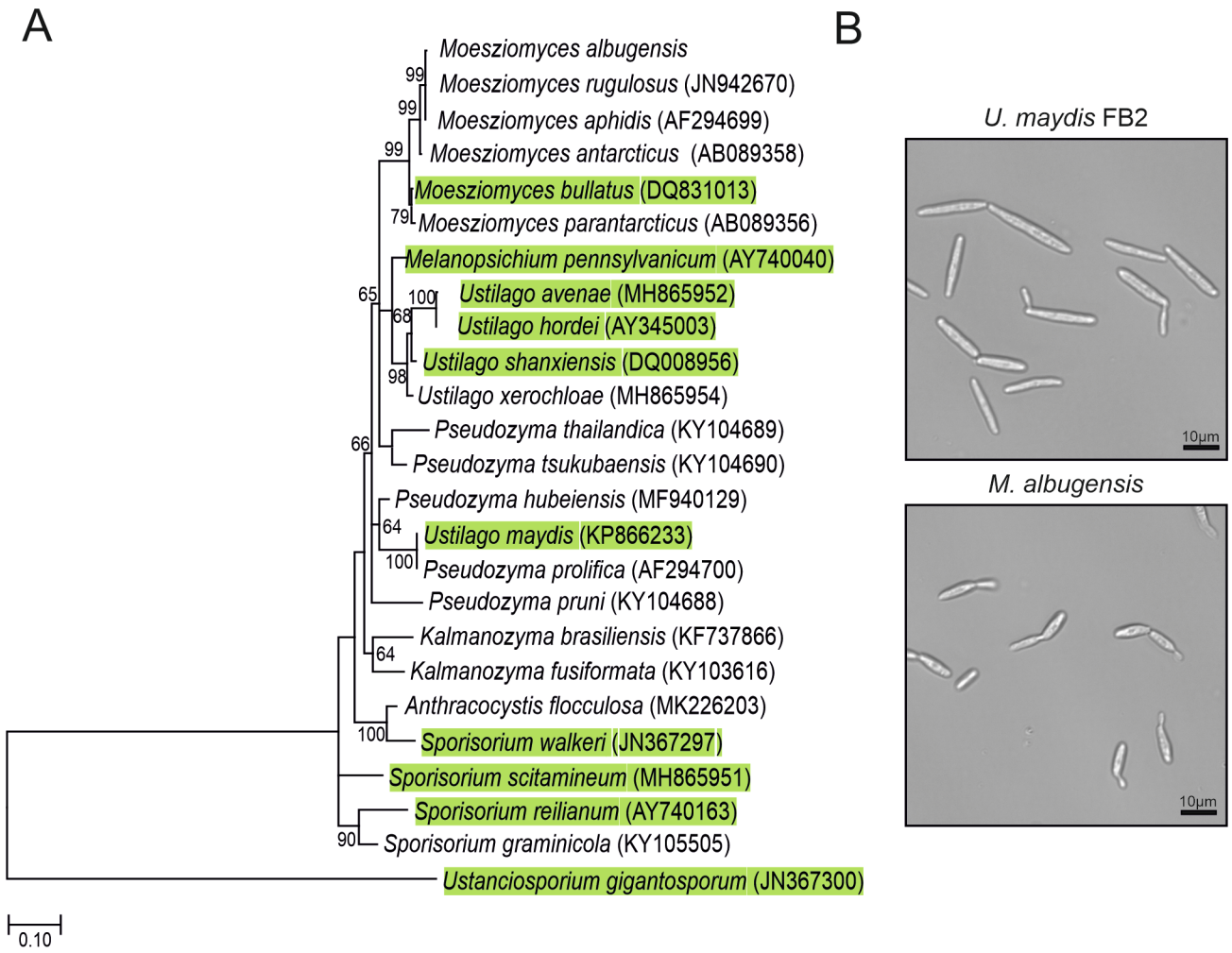

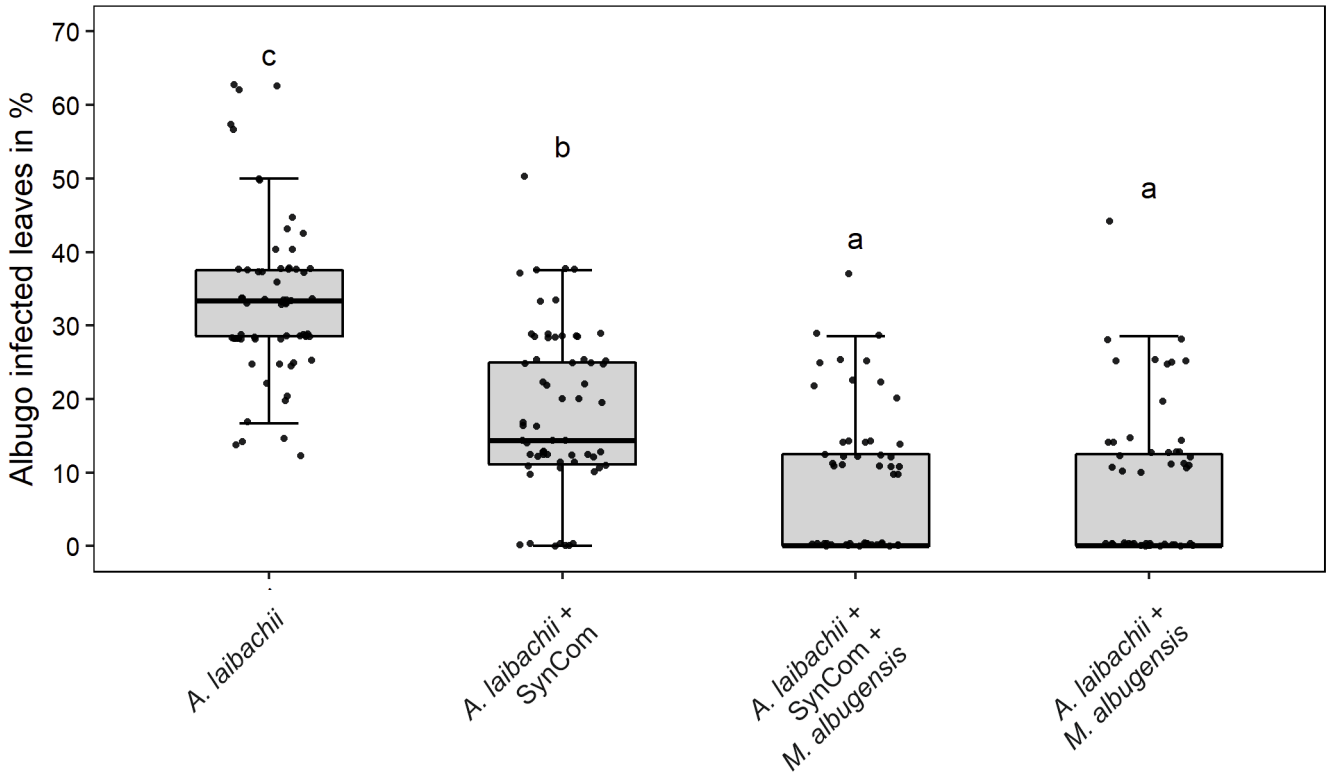

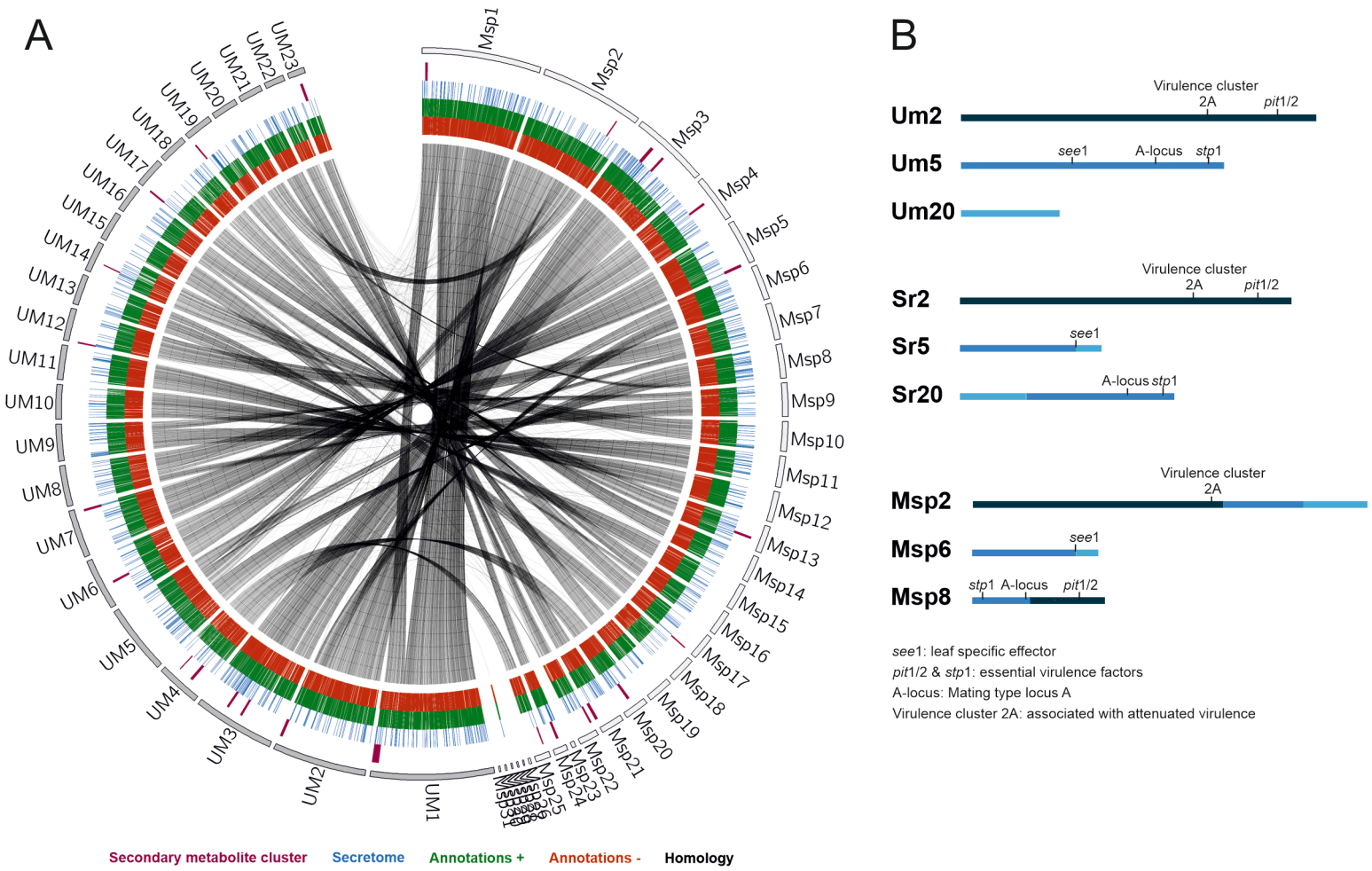

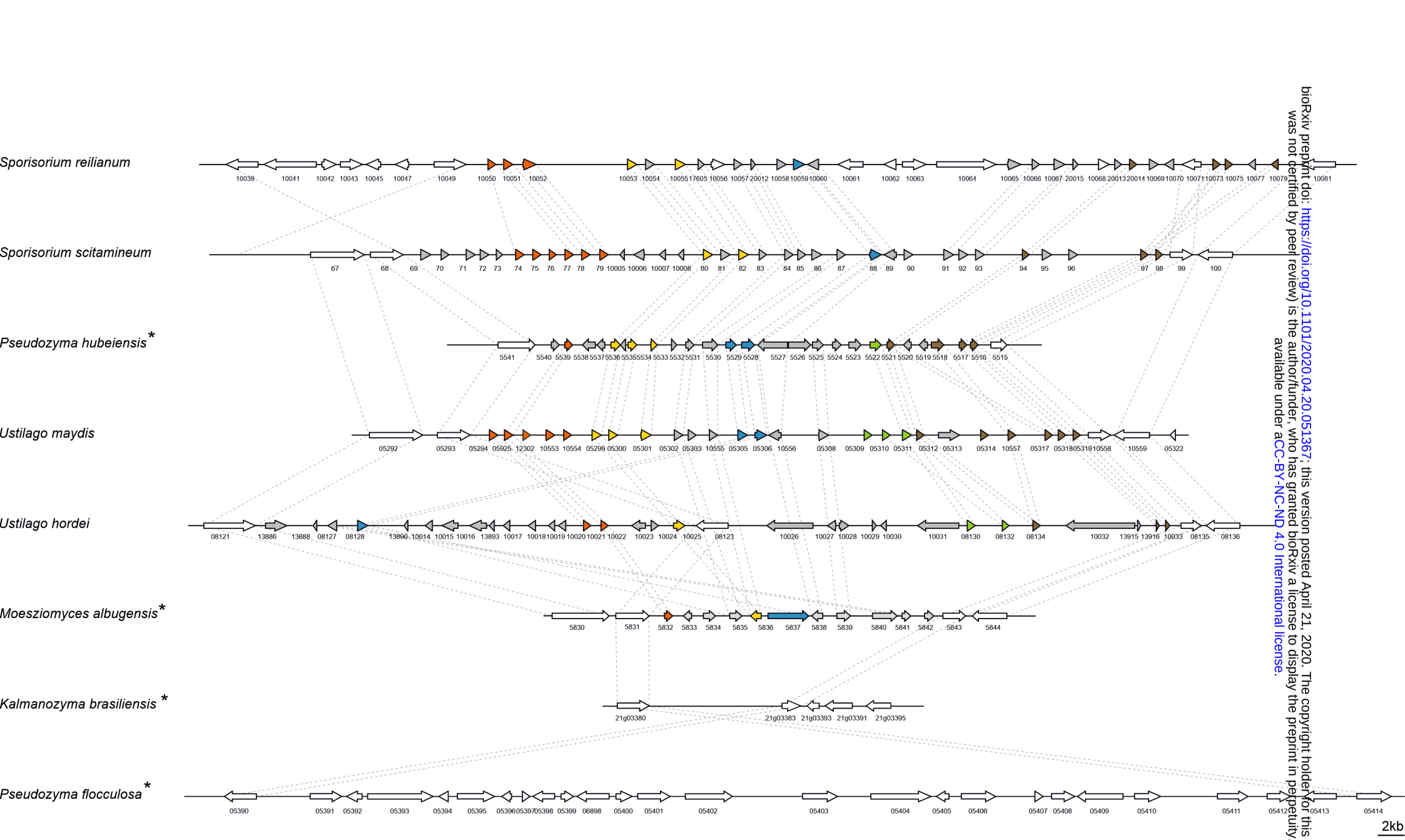

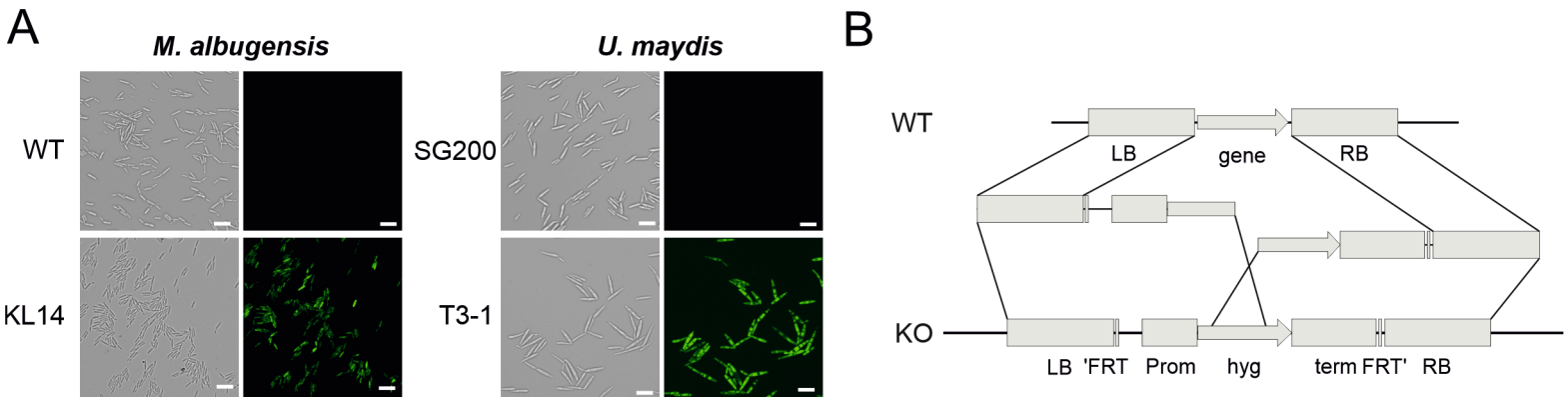

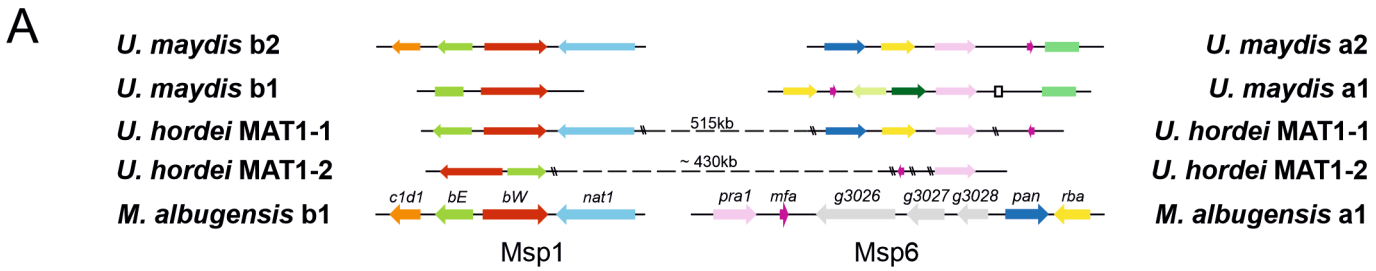

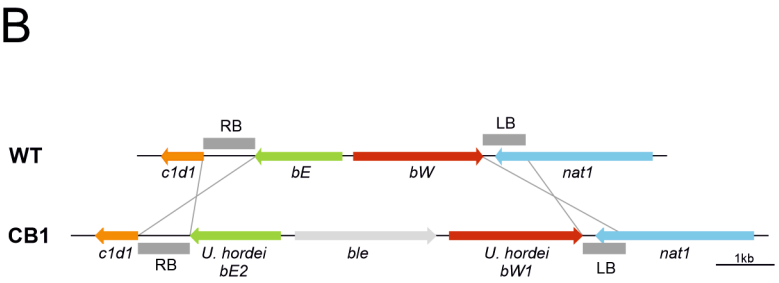

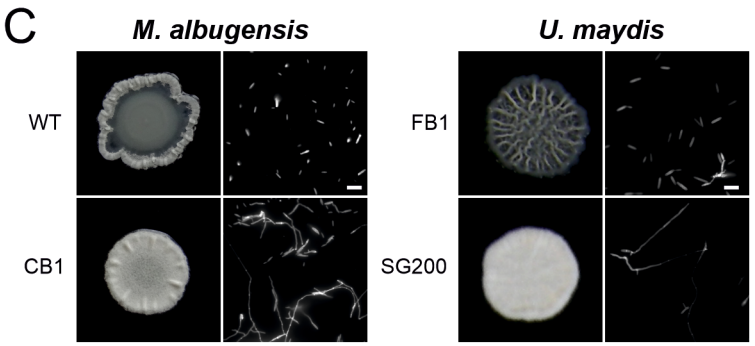

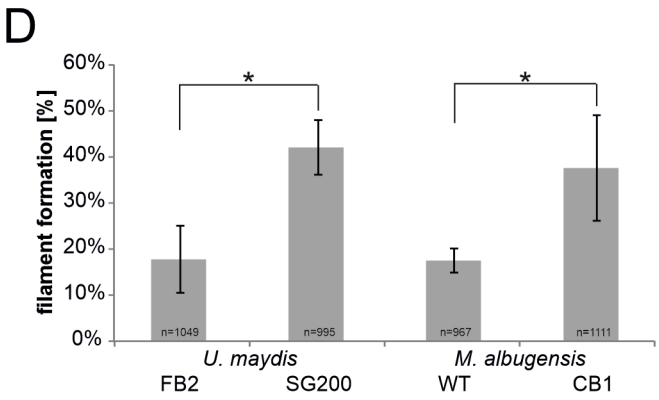

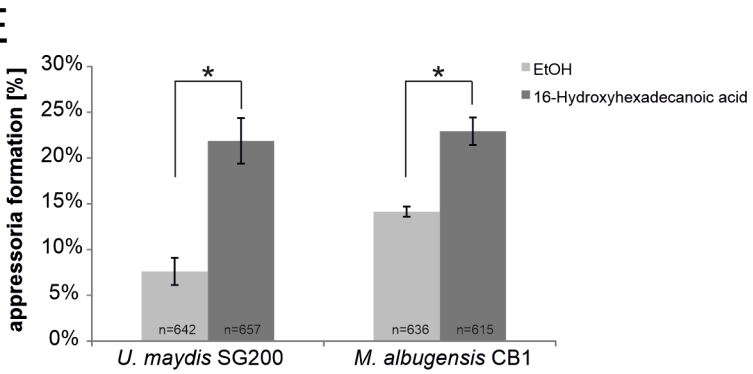

A

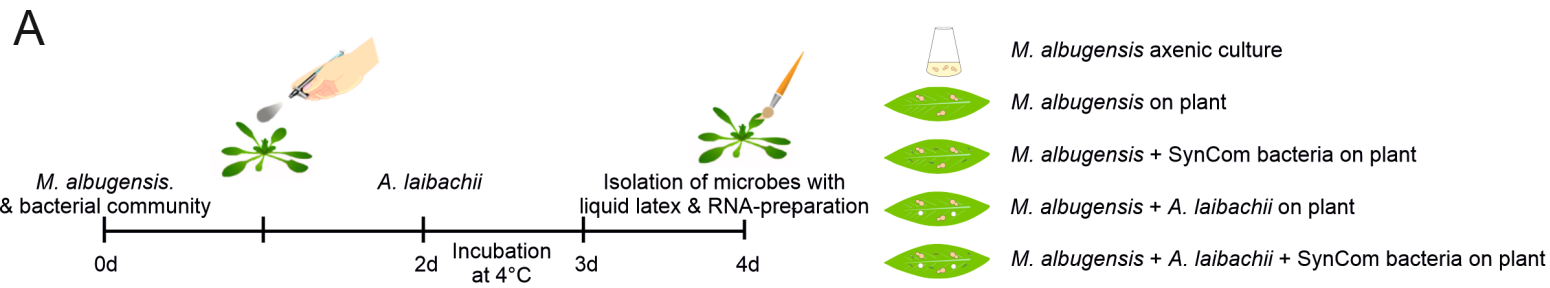

B

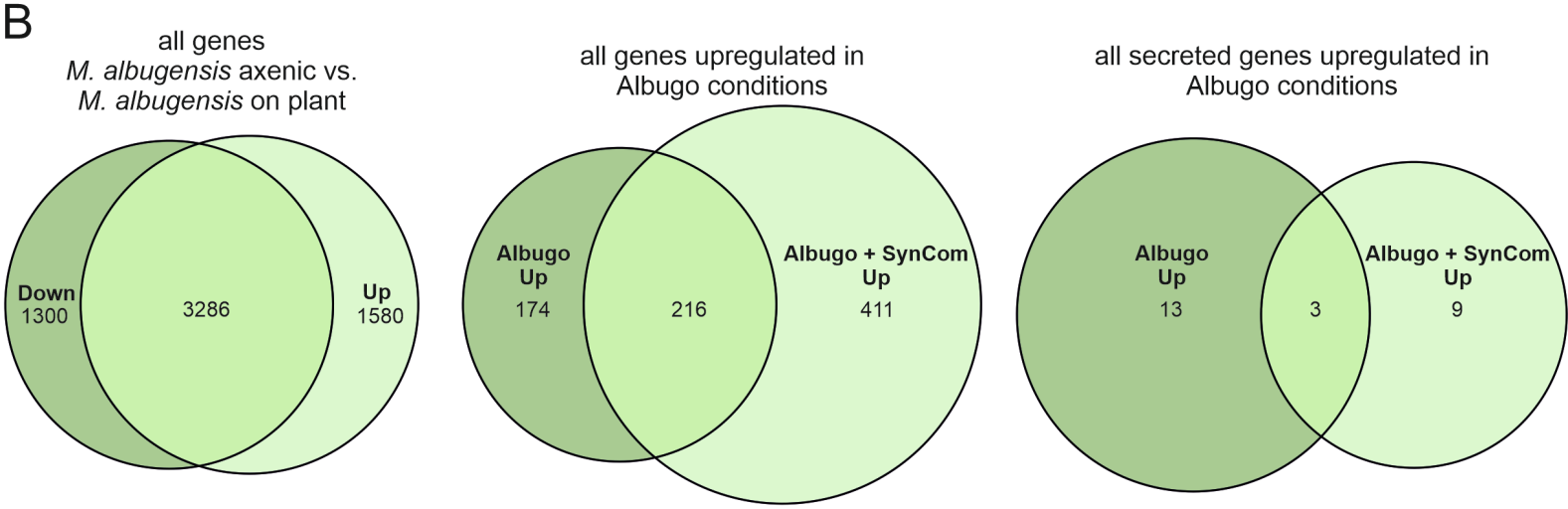

C

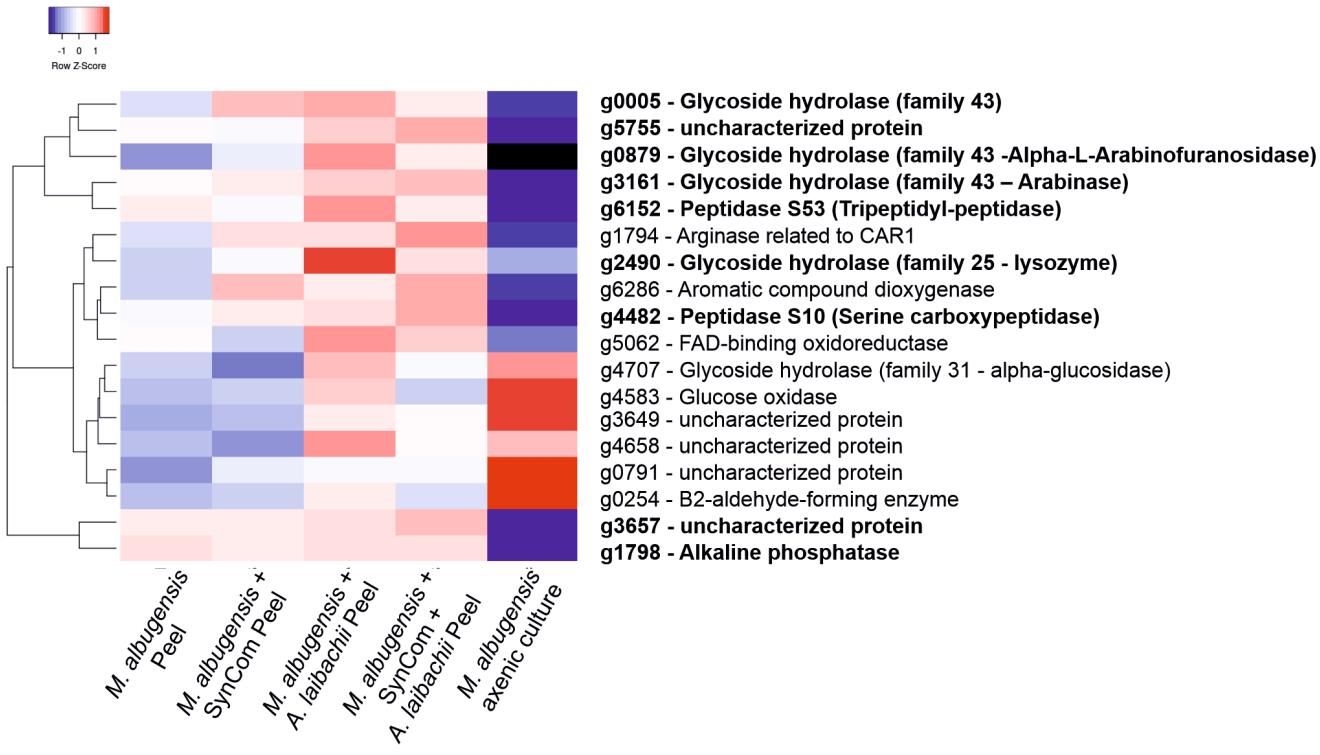

A

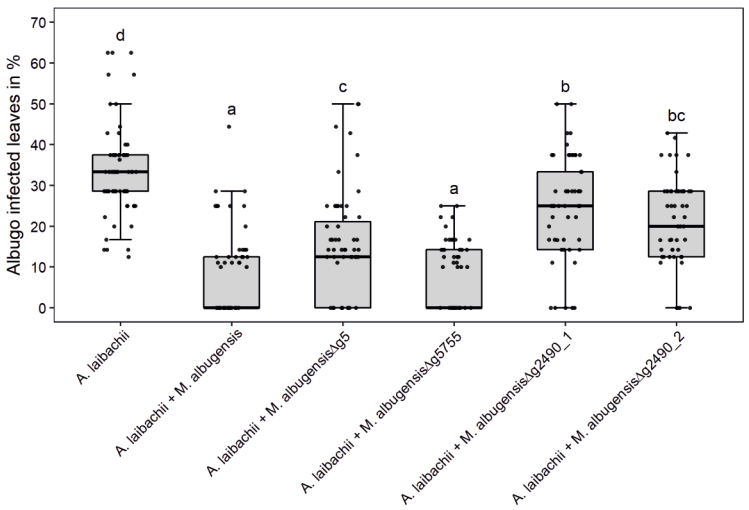

B